

## Polyimide nanocomposites prepared from high-temperature, reduced charge organoclays

D.M. Delozier<sup>a</sup>, R.A. Orwoll<sup>a</sup>, J.F. Cahoon<sup>a</sup>, J.S. Ladislav<sup>a</sup>, J.G. Smith Jr.<sup>b</sup>, J.W. Connell<sup>b,\*</sup>

<sup>a</sup>*Departments of Applied Science and Chemistry, College of William and Mary, Williamsburg, VA 23187-8795, USA*

<sup>b</sup>*NASA Langley Research Center, Advanced Materials and Processing Branch, Mail Stop 226, Hampton, VA 23681-2199, USA*

Received 7 August 2002; received in revised form 13 January 2003; accepted 14 January 2003

### Abstract

Montmorillonite clays modified with the dihydrochloride salt of 1,3-bis(3-aminophenoxy)benzene (APB) were used in the preparation of polyimide/organoclay hybrid films. Organoclays with varying surface charge based upon APB were prepared and examined for their dispersion behavior in the polymer matrix. High molecular weight poly(amide acid) solutions were prepared in the presence of the organoclays. Films were cast and subsequently heated to 300 °C to cause imidization. The resulting nanocomposite films, containing 3 wt% of organoclay, were characterized by transmission electron microscopy and X-ray diffraction. The clay's cation exchange capacity (CEC) played a key role in determining the extent of dispersion in the polyimide matrix. Considerable dispersion was observed in some of the nanocomposite films. The most effective organoclay was found to have a CEC of 0.70 meq/g. Nanocomposite films prepared with 3–8 wt% of this organoclay were characterized by transmission electron microscopy (TEM), X-ray diffraction (XRD), and thin-film tensile testing. High levels of clay dispersion could be achieved even at the higher clay loadings. Results from mechanical testing revealed that while the moduli of the nanocomposites increased with increasing clay loadings, both strength and elongation decreased.

Published by Elsevier Science Ltd.

**Keywords:** Polyimide; Nanocomposite; Organoclay

### 1. Introduction

The homogeneous dispersion of organically modified montmorillonite clays in polymer matrices can lead to physical, morphological, and mechanical-property enhancements in the resulting nanocomposites [1]. Improvements have been demonstrated with many polymer systems including polyamides [2], polystyrene [3], polymethylmethacrylate [3], polyacrylate [4], polycarbonate [5], epoxies [6], polysulfone [7], and polyurethane [8].

Naturally occurring montmorillonite exists as stacks of platelets, with thicknesses of ca. 1 nm and lateral dimensions of 100–1000 nm. A typical formulation is  $\text{Na}_{0.33}\text{Mg}_{0.33}\text{Al}_{1.67}(\text{OH})_2(\text{Si}_4\text{O}_{10})$ . Here sodium ions on the surface of each platelet balance the negative charge resulting from the substitution of lower-valence metal ions (e.g. magnesium for aluminum) in the platelets' interiors. Because of strong electrostatic forces between the layers,

unmodified clays generally disperse poorly in organic matrices. However, when the interlayer sodium ions are replaced with suitable organic cations, the surface acquires an organic character, the interlayer spacing is usually increased, and exfoliation of the platelet sheets is facilitated as polymer intercalates between the layers. Common choices for the organic surfactant are ammonium ions substituted with one or more aliphatic chains of 12 or more carbons. The ease of dispersion depends on a number of factors including the nature of the organic cation and the density of cationic sites on the platelets' surfaces.

Aromatic polyimides present unique problems as matrices for organoclay nanocomposites. Most polyimides are intractable because of their low solubilities and high softening temperatures. Thus to prepare a hybrid system the clay has to be either introduced along with the monomers before polymerization or added to a solution of the intermediate poly(amide acid). In either instance, subsequent imidization is accomplished by heating to 300 °C or higher. However, because the aliphatic-amine surfactants degrade at these high temperatures, they are not generally

\* Corresponding author. Tel.: +1-757-864-4264; fax: +1-757-864-8312.  
E-mail address: j.w.connell@larc.nasa.gov (J.W. Connell).

effective in stabilizing the clay in the polyimide matrix [9–11].

Ammonium cations with aromatic substituents, possessing greater thermal stability than their aliphatic counterparts, have also been used to render clay surfaces organophilic. They were first employed in the pesticide [12] and water-purification [13] industries. Aromatic ammonium ions were found to make clays more sorbent [14]. Using the dihydrochloride salt of 4,4'-oxydianiline (ODA) as a clay surfactant, Tyan and coworkers [15] prepared polyimide–clay nanocomposites from the same diamine (ODA) and 3,3',4,4'-benzophenonetetracarboxylic dianhydride. Other reports [16,17] from that laboratory describe studies that included the use of a thermally stable aromatic surfactant molecules including one with three quaternary amine sites.

To achieve more favorable interactions between the clay surface and the polymer, Budjak et al. [18,19] reduced the anionic character of the clay's surface by incorporating lithium ions [20,21] into the octahedral regions in the interior of montmorillonite. This lowering of the clay's cationic exchange capacity (CEC) was found to increase the affinity of poly(ethylene oxide) [18] and methylene blue [19] for the clay.

Studies on organoclay-polyimide films prepared from 1,3-bis(3-aminophenoxy)benzene (APB) and 3,3',4,4'-biphenyltetracarboxylic dianhydride, which is amorphous, are reported herein. The montmorillonite clay was modified by lowering its CEC and incorporating the dihydrochloride salt of APB as a surfactant. X-ray diffraction (XRD), transmission electron microscopy (TEM), and mechanical tests were performed to determine the effects of these clay treatments on the properties of the nanocomposite films.

## 2. Experimental

### 2.1. Starting materials

The organically modified clay (SCPX-2003) used in the preparation of nanocomposite films was purchased from Southern Clay Products, Gonzalez, TX. This organoclay consisted of a 2:1 montmorillonite modified with a quaternary ammonium salt that contained a long chain hydrocarbon (tallow) group. Cloisite ( $\text{Na}^+$ ) montmorillonite, also from Southern Clay Products, was used as received. Both clays had a CEC of 0.926 meq/g.

1,3-Bis(3-aminophenoxy)benzene [APB, Mitsui Petrochemical Ind, Ltd, melting point (m.p.) 107–109 °C] and 3,3',4,4'-biphenyltetracarboxylic dianhydride (BPDA, Chriskev Co., Inc. m.p. 295–297 °C) were obtained in polymer grade purity and used as received. All other chemicals were used as received from commercial sources.

### 2.2. Preparation of dihydrochloride salt of APB

Into a 25-ml beaker were placed APB (3 g) and 1,4-dioxane (10 ml). The mixture was stirred until the diamine completely dissolved. A 0.01N hydrochloric acid (HCl) solution was added dropwise to the APB solution while stirring until the white precipitate that formed no longer disappeared on stirring. The solution was then added to 12N HCl to ensure complete precipitation. The resulting dihydrochloride salt of APB was recovered by filtration and dried in flowing air at room temperature.

### 2.3. Preparation of reduced charge clays

Into a 1000-ml beaker were placed Cloisite  $\text{Na}^+$  (15 g) and 1000 ml of aqueous 1N lithium chloride (LiCl). The clay suspension was homogenized using a Powergen™ homogenizer for 5 min until a homogenous suspension or sol was reached. The suspension was subsequently transferred to polypropylene centrifuge tubes and centrifuged at 13,000 rpm for 10 min yielding clay pellets. The liquid was decanted. The clay was transferred to 1000 ml of a 1N LiCl solution and the suspension homogenized again. This was repeated once more making three consecutive washings. The clay was centrifuged after the last LiCl washing, separated from the liquid, and then suspended in 1000 ml deionized water via homogenization. This washing in water and subsequent centrifugation to separate the clay from the wash was repeated three times. The clay was heated in platinum crucibles in a flowing air oven for 24 h. Samples were heated to 120, 130, 140, 160, and 170 °C.

These medium-charged montmorillonite samples are designated MCM-120-Li etc., while a sample that was not heated is referred to as FCM-Li. After cooling to ambient temperature, the samples were ground to a fine powder in a ball mill.

### 2.4. Cation exchange capacity

The powdered, heat-treated lithium clay (0.2 g) and water (20 ml) were sonicated in a 50-ml polypropylene centrifuge tube until a homogenous clay–water suspension was obtained. Aqueous ammonium acetate (10 ml, 0.10N) was added dropwise. The resulting mixture was sonicated for 10 min. The clay was then compacted into a pellet by centrifugation. The clear supernatant was analyzed for lithium with atomic absorption spectroscopy. The clay was then resuspended in 20 ml of deionized water followed by sonication, treatment with 10 ml of a 0.10N ammonium acetate solution, sonication for 10 min, and centrifugation into a pellet. The supernatant was again analyzed for lithium. This cycle was repeated once more. The CEC was determined as total number of milliequivalents of lithium extracted in the three washings divided by the mass of the clay.

The exchangeable lithium content was measured on

Table 1  
Description of abbreviations

Abbreviation	Description
MCM-120-Li	Lithium treated montmorillonite clay that was held at 120 °C for 24 h
MCM-120-APB	Lithium treated montmorillonite clay that was held at 120 °C for 24 h and ion exchanged with APB <sup>+</sup>
FCM-APB	Fully charged Cloisite-Na <sup>+</sup> ion exchanged with APB <sup>+</sup>

FCM-Li, MCM-120-Li, MCM-130-Li, MCM-140-Li, and MCM-150-Li clays. The different clays are identified by the code described in Table 1.

The type of clay is mentioned first, the heating scheme is next, and the ion that is in the inner layer is last.

### 2.5. Preparation of organoclays

Into a 250-ml fleaker were placed either the Cloisite (1.00 g), or a medium-charged clay, and 100 ml of deionized water. The mixture was homogenized until a stable suspension was reached. The dihydrochloride salt of APB (0.6 g) dissolved in 20 ml of water was added dropwise to the clay suspension while sonicating. After sonication for approximately 1 h, the suspension was introduced to a Soxhlet thimble and extracted for 24 h with deionized water. The clay was lyophilized and stored in a dessicator.

### 2.6. Preparation of reference poly(amide acid) containing no clay

Into a 100-ml three-neck round-bottom flask equipped with a mechanical stirrer, nitrogen inlet, and drying tube containing calcium sulfate were placed APB (2.99 g, 0.010 mole) and 1-methyl-2-pyrrolidinone (NMP, 10 ml). The solution was stirred until the diamine completely dissolved. BPDA (3.01 g, 0.010 mole) was added as a solid followed by NMP (16 ml) to adjust the solids content to 18%. The mixture was stirred under nitrogen at room temperature for 24 h. The resulting yellow-brown solution was clear and viscous. The solution was subsequently used to prepare thin-films for characterization.

### 2.7. Preparation of poly(amide acid)/organoclay hybrids via in situ polymerization

Into a 50-ml volumetric flask were placed MCM-130-APB organoclay (0.155 g) and NMP (15 ml). The flask was fitted with a glass stopper and placed in a sonicator bath for 1 h at room temperature. The yellow-brown clay mixture was viscous and almost clear. Into a 100-ml three-neck round-bottom flask equipped with a mechanical stirrer, nitrogen inlet, and drying tube containing calcium sulfate were placed the organoclay suspension, APB (2.50 g, 8.6 mmol) and NMP (5 ml). The solution was stirred until

the diamine dissolved. Powdered BPDA (2.52 g, 8.6 mmol) and NMP (5 ml) were subsequently added. This mixture with 16% solids was stirred at room temperature for 24 h under nitrogen. The resulting amber mixture was clear and viscous. The mixture was used to prepare thin-films for characterization.

### 2.8. Thin-films

Thin-films were cast from both neat poly(amide acid) solution (reference) and poly(amide acid)/organoclay mixtures in NMP. The solution or mixture was doctored onto clean, dry plate glass and dried to a tack-free state under flowing air at room temperature in a low humidity chamber. To effect solvent removal and imidization the thermal conditions in flowing air after RT drying were 1 h each at 100, 200, and 300 °C. The films were  $30 \pm 5$  μm thick after curing. Thin-film tensile properties were determined in the doctoring direction and the transverse direction according to ASTM D882 at room temperature using five specimens for each film.

### 2.9. Other Characterization

Thermogravimetric analysis (TGA) was performed on a Seiko SSC/5200 Thermal Analyzer at a heating rate of 2.5 °C/min in air at a flow rate of 50 ml/min. TEM was obtained with a Zeiss EM109 Electron Microscope using an 80 kV accelerating voltage. For the TEM, small strips of the sample film were encased in epoxy resin prepared by curing the epoxy overnight at 80 °C. These samples were then cut using an ultramicrotome and placed on open hole copper grid coated with Formvar<sup>®</sup> for analysis. Higher magnification micrographs were obtained using a Philips CM 200 Electron Microscope using a 200 kV accelerating voltage. The grids were prepared in the same manner using 300 mesh copper grids. XRD patterns were obtained on polyimide films with a Scintag X1 X-ray diffractometer using a copper K<sub>α</sub> radiation source. XRD measurements were obtained on various orientations of the film with respect to rotation about an axis perpendicular to the plane of the film and measurements were determined to be unbiased to the direction of the film relative to the beam. Atomic absorption data was collected on a Perkin Elmer 1100B Atomic Absorption Spectrophotometer.

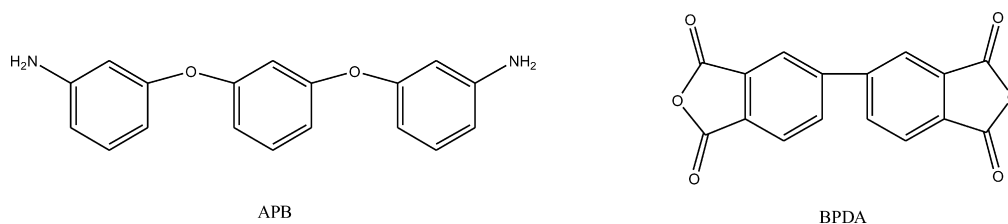


Fig. 1. Structure of monomers.

### 3. Results and Discussion

#### 3.1. Preparation of organoclays via ion exchange

The organoclays chosen for dispersion in the polyimide needed enough thermal stability to withstand the high temperature used to cure the poly(amide acid). This requirement led to the selection of aromatic molecules for surface modification of the clay. While aromatic surfactants typically form more thermally stable organoclays than aliphatic surfactants, they may be less effective than their long-chain aliphatic counterparts at promoting dispersion of the clay sheets. Modification of the surface charge on the clay and choice of an effective surfactant are also critical in the formation of organoclays. The poly(amide acid) chosen was APB-BPDA (see Fig. 1) and the dihydrochloride salt of the same APB diamine was used in the preparation of the organoclays. Based on literature reports [15,17], one end of the diamine is protonated and becomes attached to the surface of the clay while the other amino group is free to participate in the polymerization reaction.

The preparation of organoclays involved exchanging an organic ion for an inorganic ion. The amount of APB salt added was approximately a two-fold excess of the CEC of the fully charged montmorillonite (0.926 meq/g). Since the APB salt is water-soluble, the ion-exchange reactions were performed in aqueous suspensions of the sodium or lithium clay. The 1% clay suspension was converted into a sol via sonication. The clay remained suspended for hours in the absence of excess salt. The organoclays were allowed to sonicate for 1 h to ensure good mixing with the water temperature reaching 45 °C at the end of the process. Other methods of stirring, such as using a homogenizer or stirring bar, were also attempted while the salt was being added, but sonication was the most effective.

Adding the salt solution caused the clays to flocculate. With the more reduced charge clays (MCM-140, MCM-160, and MCM-170), small pellets resulted that did not stay suspended. These clays turned orange almost immediately after introduction of the APB salt then darkened after sonicating for an hour. On the other hand, the FCM, MCM-120, and MCM-130 clays became flocculant and billowy. As the APB salt was added, these clays changed slowly from colorless to orange.

The clays were washed free of excess salt by Soxhlet extraction with deionized water. They darkened in the process, apparently because of the elevated temperature. It

was later determined that temperatures above 70 °C were detrimental to the organoclay's performance. After the clays were extracted, they were lyophilized yielding an orange fluffy powder. Clays with smaller surface charges (e.g. MCM-170-APB) were darker than those with more charge (e.g. FCM-APB).

#### 3.2. Cation exchange capacity

The CECs of the heat-treated lithium clays were determined after extracting the exchangeable  $\text{Li}^+$  with ammonium acetate and measuring the milliequivalents of lithium in the wash solutions with atomic absorption. The CECs, presented in Table 2, decreased with increasing temperature. The value found for FCM-Li is larger than the CEC (0.926 meq/g) reported by the supplier for both the Cloisite ( $\text{Na}^+$ ) and the SCPX-2003 montmorillonites.

#### 3.3. Thermal analysis of organoclays

The APB organoclays were heated in air in a TGA experiment with the results presented in Table 3. The results obtained for a commercial aliphatic organoclay (SCPX-2003) are included as a comparison.

Both APB organoclays showed good thermal stability even above the 300 °C imidization temperature. In contrast, the SCPX-2003 aliphatic organoclay started degrading near 200 °C. XRD measurements on the FCM-APB and MCM-130-APB clays (described in Section 3.6 below) showed no change after heating to 300 °C following the same cure cycle used in preparing the films (Section 2.8).

#### 3.4. Preparation of polyimide/organoclay hybrids

The organoclays were combined with NMP and sonicated until they were well dispersed in the liquid. The NMP suspensions of those organoclays that had been

Table 2  
CEC values of lithium clays

Clay	CEC (meq/g) $\pm$ 0.05
FCM-Li	1.11
MCM-120-Li	0.71
MCM-130-Li	0.70
MCM-140-Li	0.63
MCM-150-Li	0.49

Table 3  
TGA data of organoclay obtained in air at a heating rate of 2.5 °C/min

Clay	Weight loss (%)			
	100 °C	200 °C	250 °C	300 °C
FCM-APB	0.00	0.00	0.33	0.68
MCM-130-APB	0.00	0.35	0.45	0.80
SCPX-2003	0.00	1.30	7.26	12.69

subjected to high temperatures (e.g. MCM-170-APB) were amber, and those clays quickly settled after sonication. In contrast, the highly charged clays (e.g. MCM-120-APB and FCM-APB) formed yellow suspensions in NMP; they remained in suspension longer and were clearer than the more reduced charge organoclay suspensions. Of all the organoclays, the MCM-130-APB suspension was the most viscous, clearest, and the most homogeneous in appearance. This clay gave the best dispersion in the polyimide (vide infra).

Polymerization to the poly(amide acid) (PAA) was carried out by first dissolving the APB diamine in the organoclay-NMP suspension and then adding BPDA (see Fig. 1) at room temperature. The different mixtures of clay and PAA varied from yellow to amber. Films were prepared from these PAA-organoclay suspensions at 3, 5, and 8 wt% clay. They varied from being clear for the FCM-APB to hazy for the MCM-170-APB. The MCM-130-APB film was translucent presumably due to light scattered by the clay particles but was not hazy. The MCM-130-APB films scattered light more intensely and were slightly more brittle with higher concentrations of clay.

### 3.5. XRD analysis of Na<sup>+</sup> clays

Samples of the MCM-120-Li, MCM-130-Li, and MCM-140-Li clays were washed with excess sodium chloride solution three times according to a literature procedure [13]

to completely replace exchangeable lithium ions with sodium. The XRD patterns of these sodium clays are compared in Fig. 2 with the XRD pattern of Cloisite (Na<sup>+</sup>) clay (FCM-Na), which had not been treated with lithium.

The MCM clays exhibited peaks near  $2\theta = 9.3^\circ$ , corresponding to a *d*-spacing of 0.95 nm. When compared to 1.34 nm for the FCM-Na Cloisite, it is apparent that the gallery spacing between the silicate sheets had been reduced considerably. Others attributed the difference to the loss of at least a monolayer of water molecules and the collapse of the gallery between the sheets [18]. Fig. 3 suggests that these layers can be fully reexpanded.

### 3.6. XRD analysis of organoclays

The diffraction patterns of the FCM-APB, MCM-120-APB, MCM-130-APB, and MCM-140-APB organoclays (Fig. 3) have maxima at  $2\theta = 6.0$ – $6.1^\circ$  (*d* = 1.46 nm). Although not shown in the figure, the analysis of the FCM-APB and MCM-130-APB organoclay after heating in the curing cycle resulted in the same peak position for the organoclay. The *d*-spacings are smaller for MCM-160-APB (1.37 nm) and MCM-170-APB (1.31 nm).

The increase in the spacings for the organoclays over their sodium counterparts is strong evidence that the inorganic cations had been successfully replaced by APB ions. The two lesser charged organoclays were found to have spacings 6–10% less than the more fully charged organoclays. This may be a consequence of (1) the reduction in the number of APB ions needed to balance the charge on the silicate surface and (2) a difference in the packing scheme due to the presence of fewer cations and a lower surface charge. The absence of peaks at  $2\theta = 9.3^\circ$  suggests that the most collapsed layers were successfully reexpanded; however, the large breadth of the basal reflection in MCM-160 and MCM-170 suggests that a mixed-layer structure consisting of expanded and collapsed layers may exist.

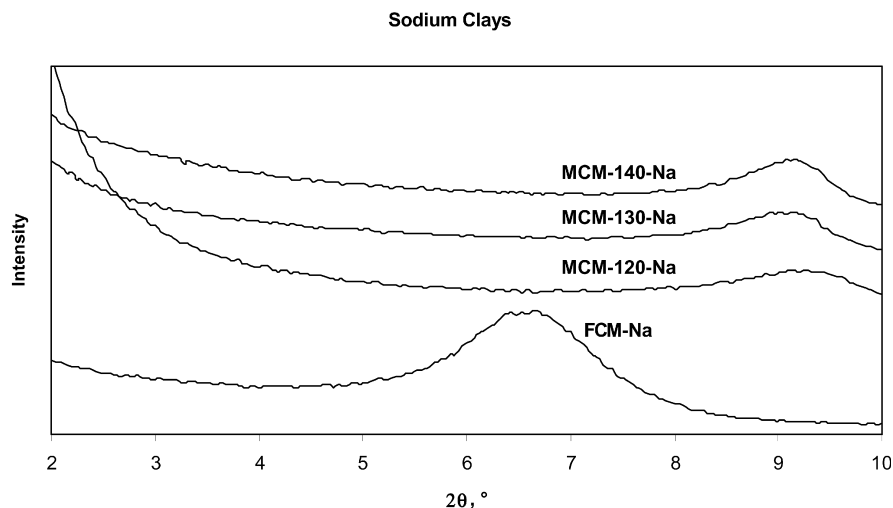


Fig. 2. XRD patterns of FCM-Na and the MCM-Na clays.



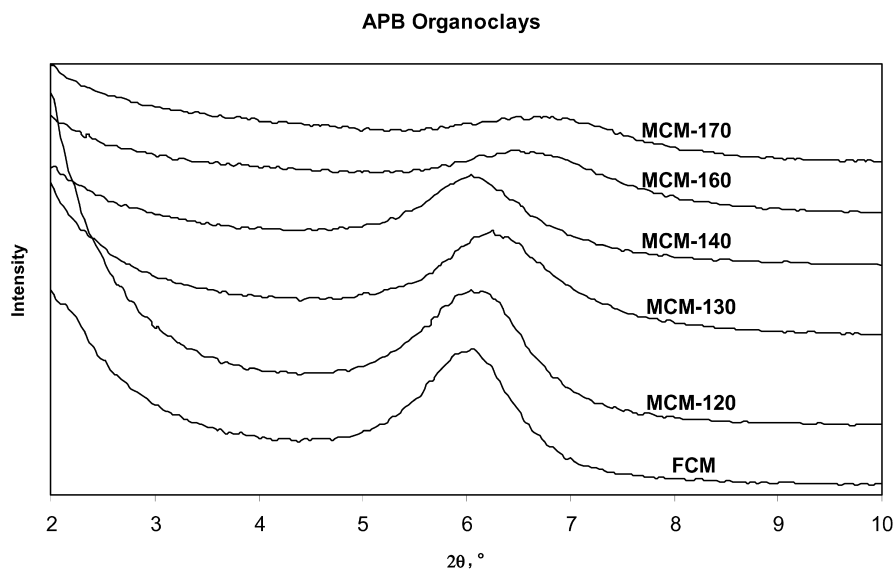


Fig. 3. XRD pattern of APB organoclays.

### 3.7. XRD analysis of APB-BPDA polyimide hybrid films containing FCM-APB and MCM-APB clays

Fig. 4 shows the XRD patterns from the hybrid films of APB-BPDA polyimides with FCM-APB and MCM-APB organoclays.

In each case the concentration of organoclay was 3 wt%. The *d*-spacings corresponding to the peaks in the XRD patterns of the films are smaller than those of the organoclays before polymerization. It is unclear why some of the clay layers collapse, but XRD experiments performed on the neat clays suggest that the collapsing is not a result of a loss of inner layer water or degradation of the surfactant cation due to overheating.

The MCM-130-APB and MCM-120-APB films were among the films containing the weakest XRD peak, thus

these may be the hybrid films with the best dispersion. The MCM-130-APB system was examined further using organoclays prepared directly from their lithium counterparts. The XRD results in Fig. 5 for the 3, 5, and 8 wt% MCM-130-APB show, for all three films, peaks from layers with a 1.28 nm spacing. The intensity of the peak increases with increasing concentration of clay. This is consistent with less agglomeration in the smaller loadings.

### 3.8. TEM Analysis of nanocomposite materials

TEM micrographs of the various nanocomposites were collected and are presented below at three different magnifications ( $3400\times$ ,  $7200\times$ , and  $22000\times$ ). The alignment of the clay platelets in one direction in some of the micrographs is most likely a result of doctoring the

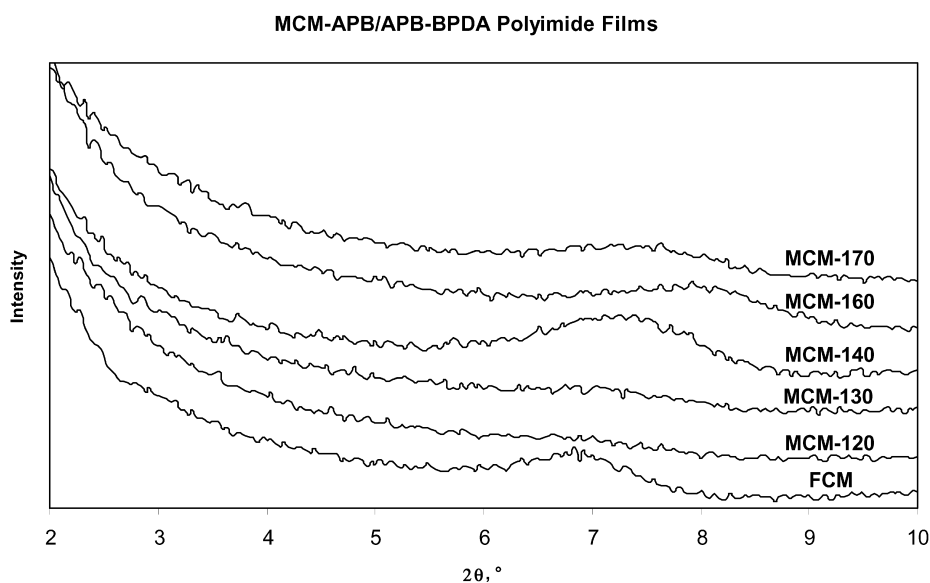


Fig. 4. XRD pattern of MCM-APB/APB-BPDA polyimide films.

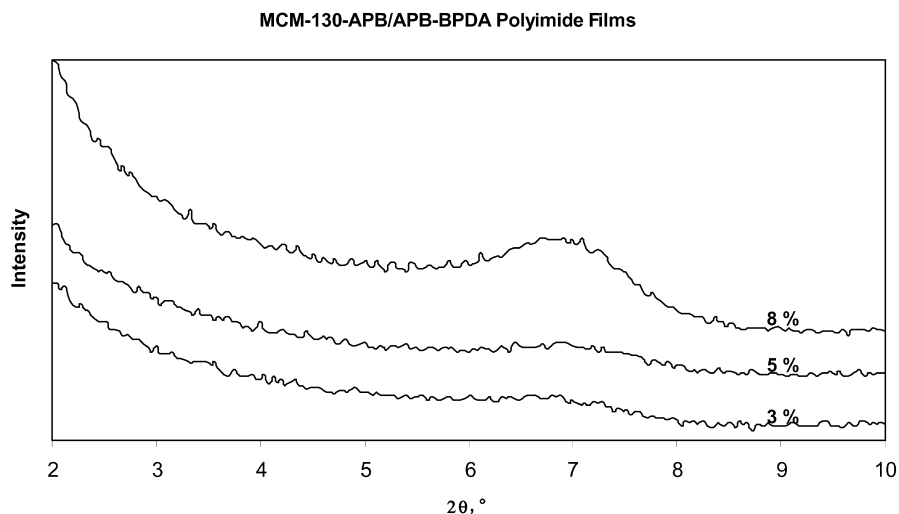


Fig. 5. XRD pattern of MCM-130-APB/APB-BPDA polyimide films.

solutions onto the glass. The number of distinguishable clay particles in the 3% samples at each magnification indicates the extent of clay dispersion. Polyimide films prepared with the fully charged FCM-APB clay were clear to the unaided eye. The TEM micrographs for this hybrid film are presented in the top row of Fig. 6 and show some dispersion although some agglomeration of the clay particles is present. Black smears most likely represent particles that were not completely perpendicular to the plane of the microtoming when the TEM sample was prepared. The bottom row of Fig. 6 shows TEM micrographs for MCM-

120-APB in APB-BPDA. The number of distinguishable clay particles apparent indicates that there are few agglomerated particles, similar to the FCM-APB film. Although it is difficult to make a conclusive comparison, both the MCM-120-APB film and MCM-130-APB film (top row of Fig. 7) seem to exhibit better dispersion than the FCM-APB film.

The micrographs obtained for MCM-130-APB organo-clay in APB-BPDA nanocomposites at loadings of 3, 5, and 8% are shown in Figs. 7 and 8. In Fig. 7 the 3% micrographs show well dispersed clay with little agglomeration and

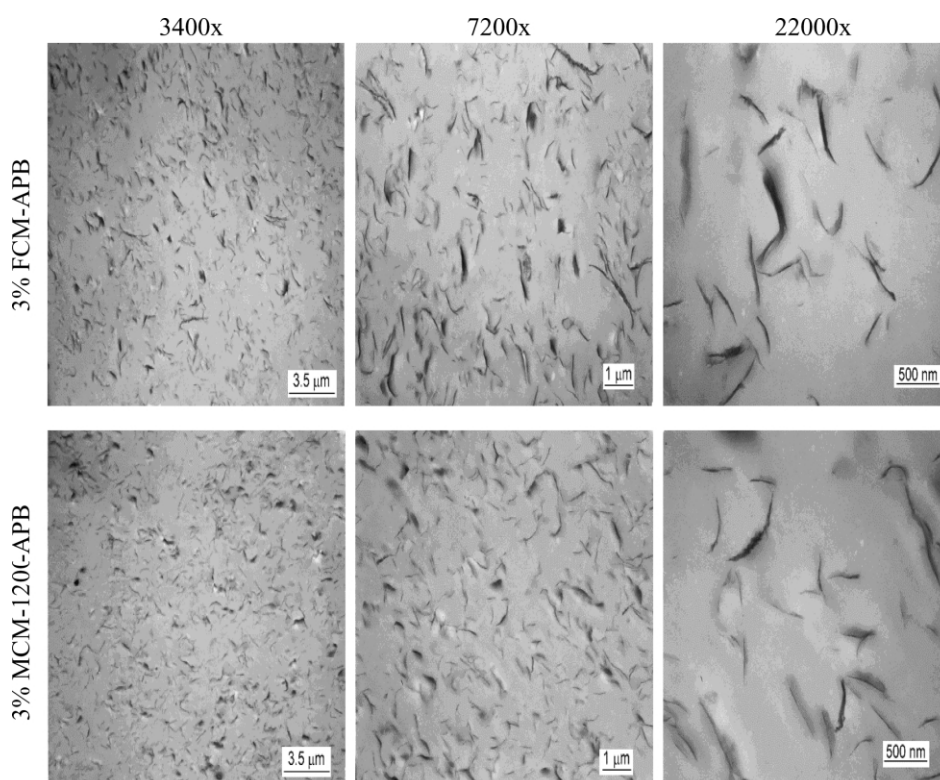


Fig. 6. TEM micrographs of 3% FCM-APB and 3% MCM-120-APB nanocomposite films.

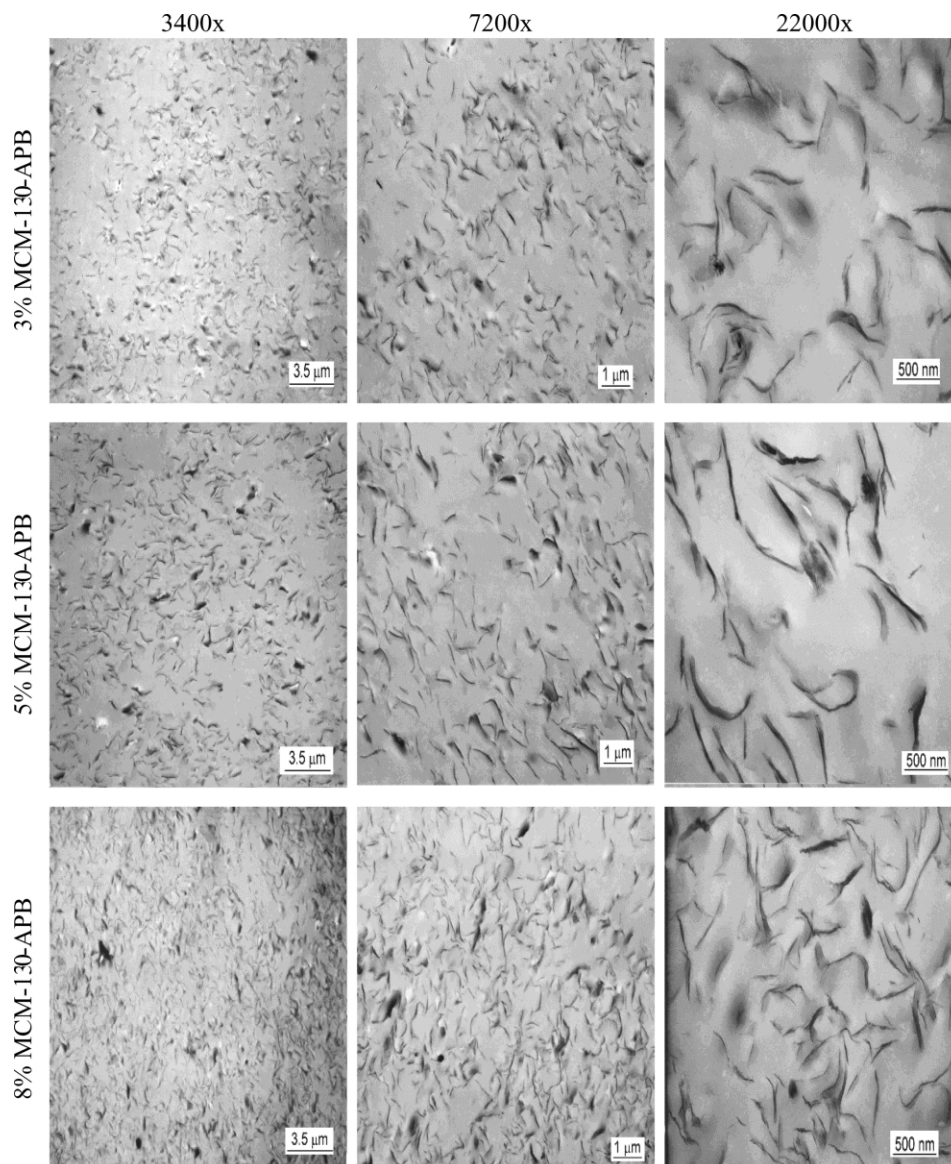


Fig. 7. TEM micrographs of 3, 5, and 8% MCM-130-APB nanocomposite films.

particles 200–700 nm in length. The 5% MCM-130-APB micrographs also show good dispersion although higher magnifications show more clay particles agglomerated into bundles. The 8% micrographs also show a high level of MCM-130-APB organoclay dispersion. The 22,000 $\times$  micrograph shows average size particles smaller than those in the 3 and 5% loaded films. The TEM micrographs suggest that a high concentration of MCM-130-APB organoclay is possible while still maintaining significant clay dispersion. In Fig. 8 the higher magnification micrographs clearly show that there are some exfoliated particles as well as some bundles. The MCM-130-APB nanocomposite films are comparable to what are considered intercalated/exfoliated by Morgan and Gilman [22].

There appears to be a relationship between a film's visual appearance and the clay charge. By the unaided eye the lower charged clays (MCM-140 through MCM-170)

apparently have more agglomerates than the more highly charged clays due to the hazy appearance of these films. Micrographs of films with MCM-140 and MCM-170 organoclays are shown in Fig. 9.

The clay exists in bundles of particles with few single clay particles and large areas where they are absent. The clays are significantly less dispersed than in the previous films, a result which can only be due to the layer charge since all other conditions were held constant.

### 3.9. Mechanical properties of APB-BPDA polyimide hybrid films containing MCM-130-APB

Thin-film tensile properties were determined in a direction transverse to the film doctoring direction. The moduli of polyimide films prepared with 3, 5, and 8 wt% loadings of MCM-130-APB were measured. As shown in



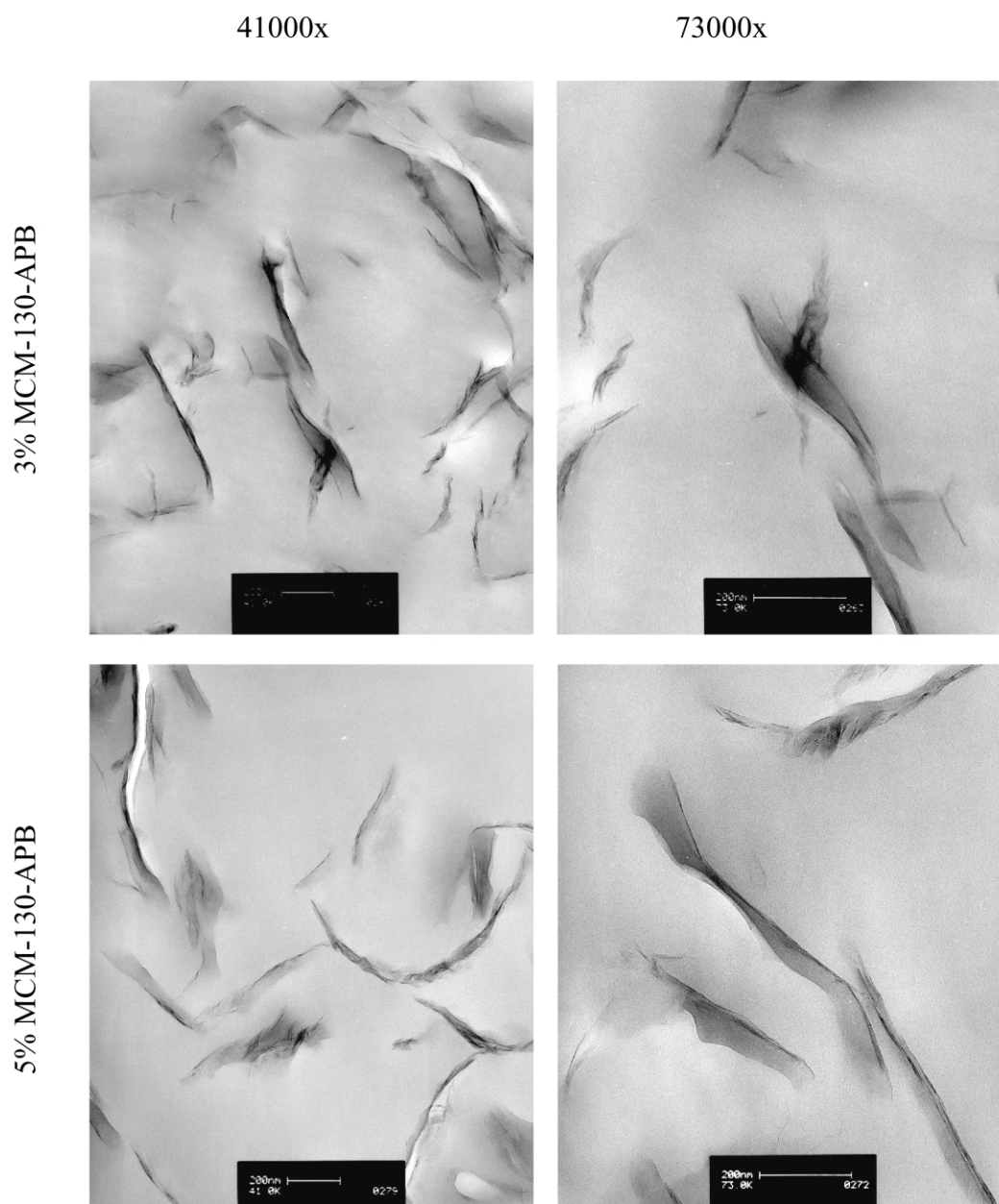


Fig. 8. High magnification micrographs of 3 and 5% MCM-130-APB nanocomposite films.

Fig. 10, they increased approximately in proportion to the concentration of clay.

The addition of clay particles to polyimides generally results in less strength [2], although strength enhancements have been reported [23]. The strengths for the three concentrations of MCM-130-APB organoclay in APB-BPDA are shown in Fig. 11. The strength decreased monotonically with the increase in clay concentration.

Elongation properties of nanocomposite materials usually follow the same trend as the strength and usually decrease at a rate that is proportional to the increase in the amount of clay that is added. This is especially true if there are clay agglomerates in the system. The data for varying percent elongation are shown in Fig. 12. As expected, the

Table 4  
Mechanical Properties of MCM-130-APB/APB-BPDA films

% Clay	Modulus (ksi)	Strength (ksi)	% Elongation
<i>Transverse</i>			
0	511	18.47	6.46
3	612	17.58	4.10
5	620	15.81	3.47
8	681	15.15	2.92
<i>Parallel (doctoring direction)</i>			
0	511	18.47	6.46
3	534	14.19	3.81
5	570	13.89	3.90
8	592	11.35	2.37

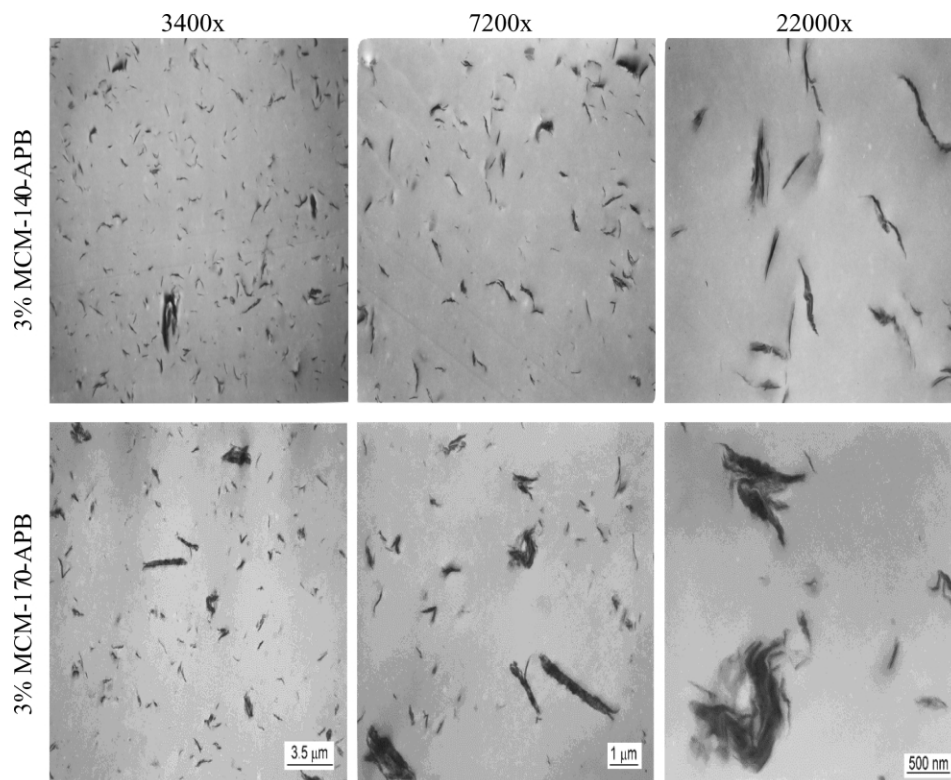


Fig. 9. TEM micrographs of 3% MCM-140-APB and MCM-170-APB nanocomposite films.

elongation properties of this material decreased as the clay concentration was increased.

Thin-film tensile properties were also determined in the direction parallel to the doctoring direction. Table 4 includes the values obtained from these experiments as well as the values obtained from above. The same general trend is followed in the mechanical properties obtained in the parallel direction, although the modulus increase is less pronounced, and the strength and elongation values are generally lower.

The mechanical properties of the nanocomposite films prepared with the other organoclays were measured. The modulus values were higher for the better dispersed clays (FCM, MCM-120-APB, and MCM-130-APB) than the films with more poorly dispersed clay (MCM-140-APB and MCM-170-APB) while the strength and elongation values increased slightly for the more poorly dispersed systems [24].

#### 4. Conclusions

Organoclays using an aromatic diamine, APB as the surfactant, were prepared and characterized. TGA analysis of the organoclay showed significantly improved thermal stability relative to that of conventional aliphatic organoclays. The surface charge of the organoclay was also modified to improve its dispersability in a polyimide matrix. Dispersion appears to be sensitive to the charge as there was only a slight difference in CEC between the MCM-130 and MCM-140 clays yet a major difference in dispersion. One composition, MCM-130, exhibited the best dispersability in APB-BPDA as evident from TEM and XRD analyses. The results from characterization suggest that when aromatic surfactants are used, increasing the lateral spacing within the galleries without significantly reducing the *d*-spacing affords conditions favorable to dispersion. Aromatic ions do

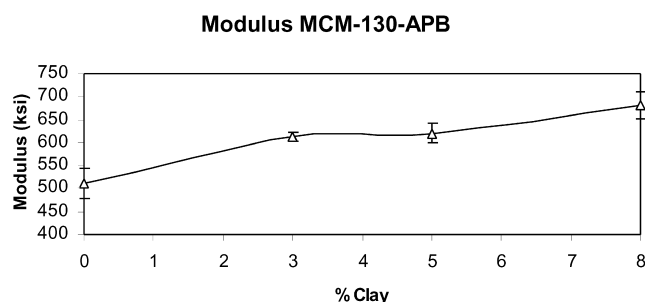


Fig. 10. Modulus of MCM-130-APB hybrid films.

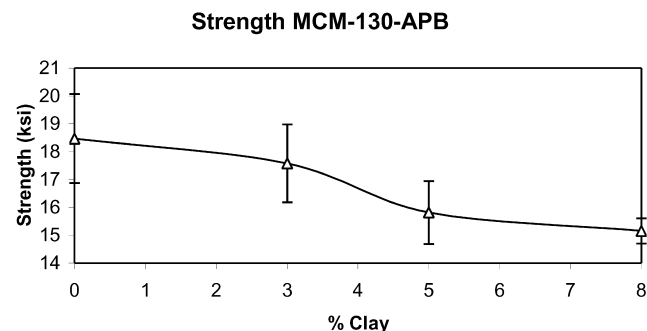


Fig. 11. Strength of MCM-130-APB hybrid films.

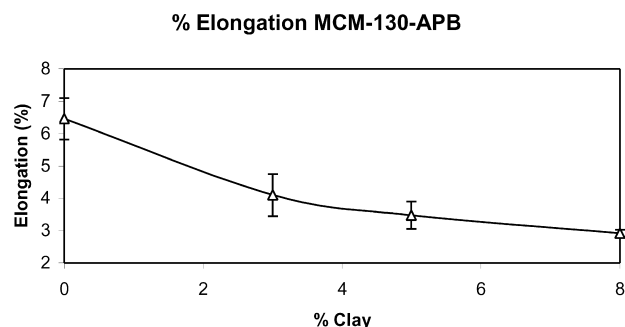


Fig. 12. Elongation of MCM-130-APB hybrid films.

not create the large *d*-spacings normally encountered in aliphatic organoclays, but good dispersion is achieved when lateral space is increased through charge reduction. Tensile testing showed that nanocomposite films prepared with the optimally charged clay exhibited some of the characteristics typically encountered in polyimide nanocomposites.

### Acknowledgements

The authors thank Ms Jewel Thomas and the Department of Biology at the College of William and Mary for assistance in obtaining TEM micrographs and Patrice Mason at the Virginia Institute of Marine Science (VIMS) for also assisting in obtaining TEM micrographs. High magnification TEM was done at NASA by Dr Roy Crooks. The authors thank VIMS for allowing use of the XRD. The authors also thank Southern Clay Products for their gracious donation of clay used for this study.

### References

- [1] Biswas M, Ray SS. *Adv Polym Sci*. 2001;155:167.
- [2] Okado A, Kawasumi M, Kojima Y, Kurauchi T, Kamigato O. *Mater Res Soc Symp Proc* 1990;171:45.
- [3] Okamoto M, Morita S, Taguchi H, Kim Y, Kotaka T, Tateyama H. *Polymer* 2000;41:3887–90.
- [4] Chen Z, Huang C, Liu S, Zhang Y, Gong K. *J Appl Polym Sci* 2000;75:796–801.
- [5] Vaia R, Huang X, Lewis S, Brittain W. *Macromolecules* 2000;33:2000–4.
- [6] Lan T, Kaviartna P, Pinnavaia T. *Proceedings of the ACS PMSE* 1994;71:527–8.
- [7] Sur G, Sun H, Lyu S, Mark J. *Polymer* 2001;42:9783–9.
- [8] Wang Z, Pinnavaia T. *Chem Mater* 1998;10:3769–71.
- [9] Delozier D, Orwoll R, Cahoon J, Johnston N, Smith J, Connell J. *Polymer* 2002;43:813–22.
- [10] Yang Y, Zhu Z, Yin J, Wang X, Qi Z. *Polymer* 1999;40:4407–14.
- [11] Xie W, Gao Z, Pan W, Vaia R, Hunter D, Singh A. *Polym Mater Sci Engng Proc* 2000;82:284–5.
- [12] El-Nahhal Y, Nir S, Serban C, Rabinovitch O, Rubin B. *J Agric Food Chem* 2000;48:4791–801.
- [13] Stevens J, Anderson S. *Clays Clay Miner* 1996;44:132–41.
- [14] Jaynes W, Vance G. *Clays Clay Miner* 1999;47:358–65.
- [15] Tyan H, Wei K, Hsieh T. *J Polym Sci, Part B: Polym Phys* 2000;38:2873–8.
- [16] Tyan H, Leu C, Wei K. *Chem Mater* 2001;13:222–6.
- [17] Tyan H, Wei K, Hsieh T. *Chem Mater* 1999;11:1942–7.
- [18] Budjak J, Hackett E, Gianellis E. *Chem Mater* 2000;12:2168–74.
- [19] Budjak J, Komadel P. *J Phys Chem B* 1997;101:9065–8.
- [20] Hoffman U, Klemen RZ. *Anorg Allg Chem* 1950;262:95–9.
- [21] Jaynes WE, Bigham JM. *Clays Clay Miner* 1987;35:440–8.
- [22] Morgan A, Gilman J. *J Appl Polym Sci* 2003;87:1329–38.
- [23] Chang J, Park D, Ihn K. *J Appl Polym Sci* 2002;84:2294–301.
- [24] Delozier D. Preparation and characterization of polyimide/organoclay nanocomposites. PhD thesis, The College of William and Mary.